Wireless Personal Communications (2021) 117:1527–1536
https://doi.org/10.1007/s11277-020-07933-8

Miniaturized Harmonic Suppressed Wilkinson Power Divider using Lumped Components and Resonators

Masoud Heydari[1] · **Saeed Roshani**[2]

Accepted: 29 October 2020 / Published online: 21 November 2020

Abstract
In this article, a miniaturized and harmonics suppressed Wilkinson power divider (WPD) is analytically designed. In the proposed divider composite transmission lines and resonator cells are utilized to eliminate unwanted harmonics and reduce circuit size. This structure has a 52% size reduction, compared to the typical WPD. According to the measured results, more than 22, 42, 45 and 40 dB suppression for 3rd, 4th, 5th and 6th harmonics are achieved. The presented WPD has lower than 0.15 dB insertion loss, more than 30 dB output ports isolation and more than 20 dB return losses in all ports at the operating frequency of 1.5 GHz is obtained.

Keywords Composite transmission line · Harmonic suppressed · Insertion loss · Power divider · Resonator cell · Size reduction

1 Introduction

Nowadays, microwave and radio-frequency devices are widely used in various applications [1–5]. The design of miniaturized devices is an important demand for modern wireless networks. Dividers are important components in the recent RF circuits and systems such as frequency multipliers, mixer and power amplifiers [6]. Recently, design a miniaturized power divider with harmonics rejections is an important challenge. So far, different methods are introduced, to reduce the circuit size of power dividers [7–10]. Using non-uniform transmission lines (TLs) instead of usual uniform TLs in [7], leads to decrease the overall size of the reported divider up to 52% compared to the conventional divider. In [8], coupled line sections are used to decrease the size of the power divider. Using microstrip EBG cell [9] and defected ground structure (DGS) [10], are also another methods to achieve size reduction, which are difficult to implement and not suitable methods to reduce the circuit size [11].

✉ Saeed Roshani
s_roshany@yahoo.com

1 Young Researchers and Elite Club, Kermanshah Branch, Islamic Azad University, Kermanshah, Iran

2 Department of Electrical Engineering, Kermanshah Branch, Islamic Azad University, Kermanshah, Iran

Compact resonators [12–16], low-pas filters [17–22] and band-pass filters [23–25] can be used in the dividers structure for size reduction and harmonics suppression purposes. Unfortunately, this method increases the insertion loss in the pass-band.

Stub-loaded resonators in the reported structure in [26], resulted in 20 dB suppression for the 2nd and 3rd harmonics, besides size reduction. Using a coupling structure instead of the traditional quarter-wavelength lines in [27] resulted in a wide harmonics rejection band.

In some recent works, artificial intelligence and neuro-based approaches are used to design optimum devices [28–30].

In this work, a miniaturized WPD with unwanted harmonics elimination is proposed. Composite transmission lines and resonator cells are used instead of bulky quarter wavelength transmission lines, which occupied large areas in the conventional divider. Furthermore using this technique, not only eliminates unwanted harmonics with good attenuation level, but also reduces 52% of the occupied area compared to the conventional one at the main frequency of 1.5 GHz. Section II of the paper will present theoretical design procedures. Simulation and experimental results are expressed in section III. The conclusion of the paper is presented in section IV.

2 Design Procedure

In this design, an equal Wilkinson power divider is proposed based on the unequal divider structure. Figure 1a demonstrates, the conventional equal WPD. In the conventional structure, two long quarter-wavelength microstrip branches ($\sqrt{2}Z_{01}$) and a lumped resistor ($2Z_{01}$) exist. Figure 2b, depicts the structure of the conventional unequal divider. If the power division ratio (k) in the unequal divider is 1, it becomes an equal one. The unequal divider consists of two microstrip lines between the input port and an isolation resistor and two lines between output ports and isolation elements. The characteristic impedance values of each line and isolation resistor value are discussed in [6].

The block diagram schematic of the proposed WPD is demonstrated in Fig. 1c. The proposed divider consists of four short transmission lines, two inductors, two resonator cells,

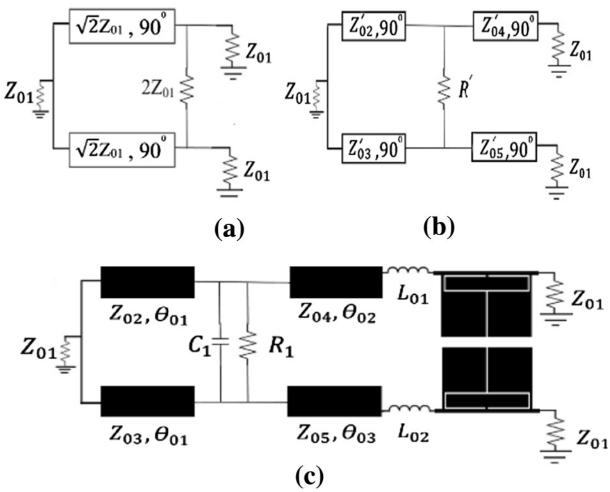

Fig. 1 Wilkinson power divider **a** equal conventional, **b** unequal conventional, **c** proposed one

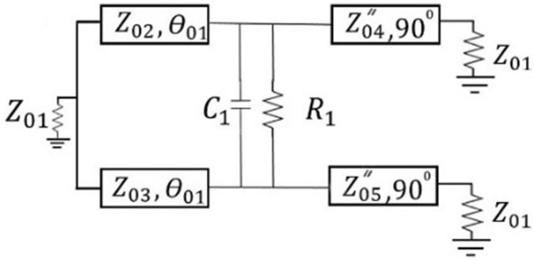

Fig. 2 The block diagram of the primitive power divider

a capacitor and a resistor to isolate output ports. The design procedure and analysis of the proposed divider, has three parts. At first, the primitive structure (part I) is designed and explained, then long λ/4 branches are replaced by composite lines (part II). At the end (part III) resonator cells are used instead of output microstrip lines.

2.1 The Primitive Divider Structure (Part I)

The conventional unequal divider as shown in Fig. 1b, which occupied large areas, because of large input microstrip transmission lines. According to the reported method in [31] the primitive power divider is designed. The block diagram of the primitive divider is illustrated in Fig. 2. Characteristic impedances of the primitive divider could be defined as follows:

$$Z_{02} = Z_{03} = 2Z_{01} \tag{1}$$

$$Z''_{04} = Z''_{05} = \sqrt{2}Z_{01} \tag{2}$$

$$R_1 = 4Z_{01} \tag{3}$$

$$C_1 = \frac{1}{4Z_{01}\omega \tan\theta} \tag{4}$$

where ω is the operation angular frequency. The C_1 and R_1 are capacitor and resistor, which are used to output ports isolation.

2.2 Composite Transmission Lines (Part II)

In order to have more size reduction, output applied transmission lines (shown in Fig. 2), which occupied large areas are replaced by equal composite transmission lines with compact size as shown in Fig. 3.

According to the ABCD matrix discussed in [6], the transmission matrix of each section in Fig. 3 can be expressed as follows:

$$[\mathrm{ABCD1}] = \begin{bmatrix} 0 & jz \\ \frac{j}{z} & 0 \end{bmatrix} \tag{5}$$

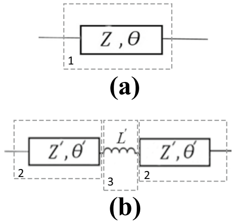

Fig. 3 **a** Conventional transmission line and its, **b** equivalent composite transmission lines

$$[\mathrm{ABCD2}] = \begin{bmatrix} \cos\theta' & \mathrm{j}z'\sin\theta' \\ \frac{j}{z'}\sin\theta' & \cos\theta' \end{bmatrix} \tag{6}$$

$$[\mathrm{ABCD3}] = \begin{bmatrix} 1 & \mathrm{j}\omega\mathrm{L}' \\ 0 & 1 \end{bmatrix} \tag{7}$$

Equating, the [ABCD] matrices of the composite transmission lines in Fig. 3b with the conventional transmission line, in Fig. 3a, resulted as:

$$[\mathrm{ABCD}_1] = [\mathrm{ABCD}_2] \times [\mathrm{ABCD}_3] \times [\mathrm{ABCD}_2] \tag{8}$$

$$\begin{bmatrix} \cos\theta' & jz'\sin\theta' \\ \frac{j}{z'}\sin\theta' & \cos\theta' \end{bmatrix} \times \begin{bmatrix} 1 & j\omega L' \\ 0 & 1 \end{bmatrix} \times \begin{bmatrix} \cos\theta' & jz'\sin\theta' \\ \frac{j}{z'}\sin\theta' & \cos\theta' \end{bmatrix} = \begin{bmatrix} 0 & jz \\ \frac{j}{z} & 0 \end{bmatrix} \tag{9}$$

$$\begin{bmatrix} \cos^2\theta' \_ \frac{j}{z'}\sin\theta'\cos\theta' \_ \sin^2\theta' & 2jz'\sin\theta'\cos\theta' + j\omega L'\cos^2\theta' \\ \frac{1}{2}\sin\theta'\cos\theta' \_ \frac{j\omega L'}{z'^2}\sin^2\theta' + \frac{j}{z'}\sin\theta'\cos\theta' & j\sin^2\theta' \_ \frac{\omega L'}{z'}\sin\theta'\cos\theta' + \cos^2\theta' \end{bmatrix} = \begin{bmatrix} 0 & jz \\ \frac{j}{z} & 0 \end{bmatrix} \tag{10}$$

After some algebraic calculations, the characteristic impedance (Z'), electrical length (θ') of the composite transmission line and lumped inductance (L') have been obtained as below:

$$\omega\mathrm{L}' = \frac{2\mathrm{z}'}{\tan 2\theta'} \tag{11}$$

$$\mathrm{z}' = \mathrm{z}\tan\theta' \tag{12}$$

Figure 4, shows the structure of power divider using composite transmission lines. The characteristic impedance of Z_{04}, Z_{05} and lumped elements values L_{01}, L_{02} are calculated based on (11–12). In this design θ_{02} and θ_{03} are considered equal.

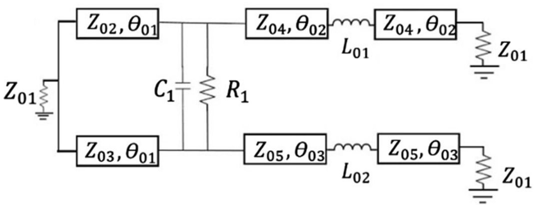

Fig. 4 Structure of the power divider using composite transmission lines

$$Z_{04} = Z_{05} = \sqrt{2}Z_{01}\tan\theta_{02} \tag{13}$$

$$L_{01} = L_{02} = \frac{2Z_{05}}{\omega\tan 2\theta_{02}} \tag{14}$$

2.3 Proposed Resonator Cells (Part III)

In order to eliminate unwanted harmonics, the designed resonator is proposed as depicted in Fig. 5a. The scattering parameters of this cell are depicted in Fig. 5b.

The size dimensions of proposed resonator cell based on RO4003 substrate with 20 mil thickness and dielectric constant of 3.38, are shown in Fig. 5, which listed as follows: $L_1=6.4$, $L_2=6.2$, $L_3=0.2$, $L_4=3.5$, $L_5=0.3$, $W_1=2.4$, $W_2=3.3$, $W_3=0.7$ and $W_4=0.2$ (all in mm). The all gaps between microstrip lines in proposed resonator are 0.1 mm.

Fig. 5 The proposed resonator cell **a** layout, **b** frequency response

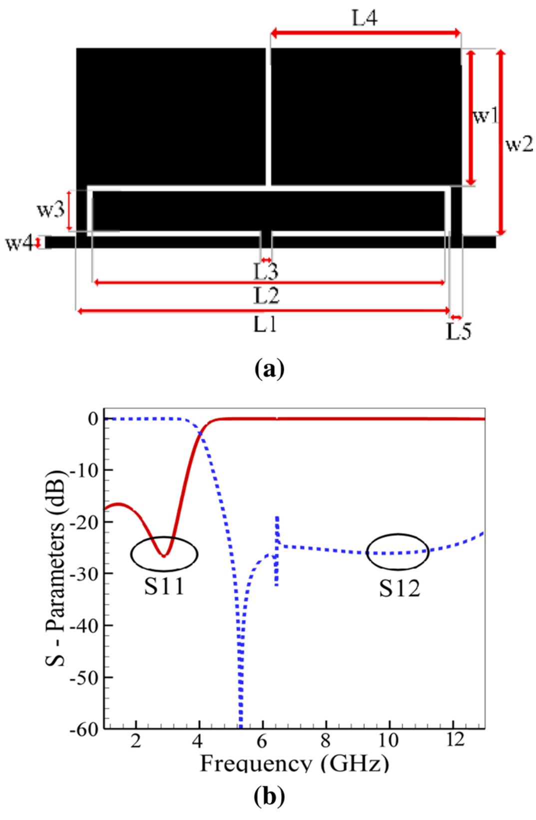

3 Experimental Results and Simulation

Figure 6a shows the structure of the proposed WPD. The layout of the square shaped and circular shaped of the conventional WPDs, are demonstrated in Fig. 6b, c respectively. According to (1)–(4) and (13)–(14) with little optimization, the electrical lengths and characteristic impedances of the proposed divider are obtained as follows: $Z_{01} = 50\ \Omega$, $Z_{02} = 100\ \Omega$, $Z_{04} = 29\ \Omega$, $L_{01} = L_{02} = 6.1$ nH, $C_1 = 3.6$ pF, $R_1 = 200\ \Omega$, $\theta_{01} = 9.25°$ and $\theta_{02} = 22.5°$.

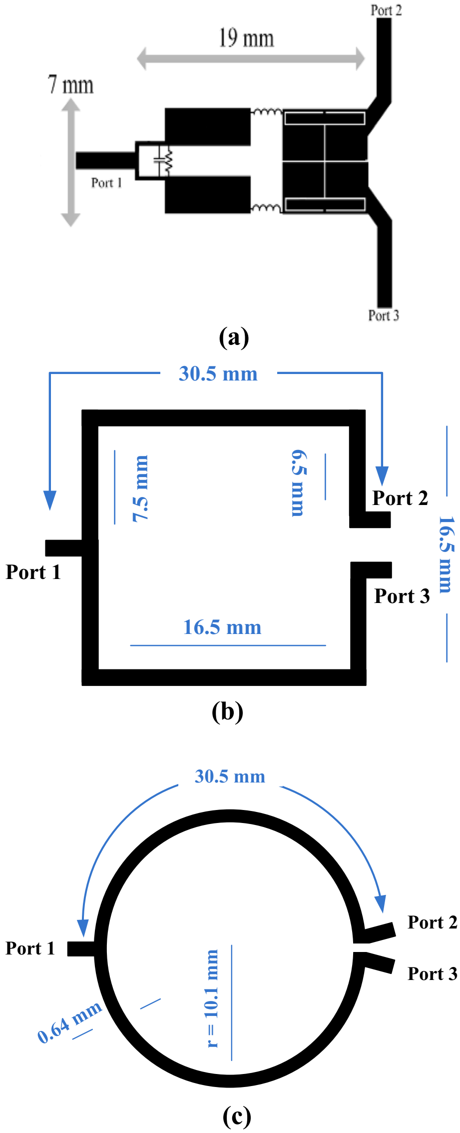

Fig. 6 Wilkinson power divider **a** layout of the proposed, **b** layout of the square-shaped and **c** circular-shaped of the conventional

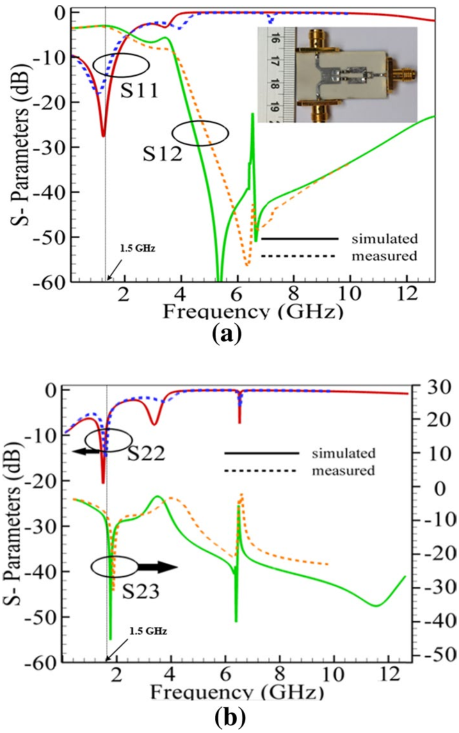

Fig. 7 Simulated and measurement results of designed WPD **a** input return loss and Insertion loss, **b** isolation and output return losses

The proposed divider is fabricated on RO4003 substrate (H = 20 mil, $\mathscr{E}_r$ $\mathscr{E}$= 3.38 and tanα = 0.0022). The measurement and electromagnetic (EM) simulation curves of the designed WPD are depicted in Fig. 7a, b. As seen in Fig. 7a, the obtained values of S_{12} and S_{13} are − 3.15 dB. The input return loss is more than 20 dB at operating frequency and harmonics suppression is up to 10 GHz with a more than 20 dB suppression level. As seen in Fig. 7b, more than 20 dB output return losses and better than 30 dB output ports isolation are obtained at 1.5 GHz. The overall circuit size of the proposed WPD is only 0.15 × 0.05 λg, which shows more than 52% size reduction compared to the typical WPD.

A performance comparison between some related WPDs and the proposed divider are listed in Table 1. The proposed WPD has a small area compared with other reported works and also has very good harmonics suppression performance.

4 Conclusion

A compact Wilkinson power divider using lumped component elements and resonator cells for harmonics suppression has been described. The proposed divider has more than 52% size reduction compared to the conventional WPD. More than 20 dB return losses at all input and output ports and better than 30 dB output ports isolation are obtained at 1.5 GHz for the fabricated device.

Table 1 Performance comparison between proposed WPD and other works

Refs.	Parameters					
	freq. (GHz)	Nth harmonics suppression		Reduction size (%)	FBW (%)	Applied technique
[26]	2.4	2nd	> 20 dB	–	28	Resonator cell
		3rd	> 20 dB			
[32]	1.5	3rd	> 20 dB	15.6	–	Lumped capacitor
		4th	> 20 dB			
[33]	1	2nd	28 dB	60	27	Lumped inductor
		3rd	32 dB			
		4th	20 dB			
[34]	1.65	3rd	45 dB	35	22	Open stub
		5th	43 dB			
This work	1.5	3rd	26 dB	52	28	Lumped element, resonator cell
		4th	43 dB			
		5th	41 dB			
		6th	37 dB			

References

1. Hong, J. S., & Lancaster, M. J. (2004). *Microstrip filters for RF/microwave applications*. New York: Wiley.
2. Melati, D., Waqas, A., Mushtaq, Z., & Melloni, A. (2017). Wideband integrated optical delay line based on a continuously tunable Mach–Zehnder interferometer. *IEEE Journal of Selected Topics in Quantum Electronics, 24*(1), 1–8.
3. Caloz, C., & Itoh, T. (2005). *Electromagnetic metamaterials: Transmission line theory and microwave applications*. New York: Wiley.
4. Waqas, A., Melati, D., & Melloni, A. (2018). Cascaded Mach–Zehnder architectures for photonic integrated delay lines. *IEEE Photonics Technology Letters, 30*(21), 1830–1833.
5. Waqas, A., Melati, D., & Melloni, A. (2018). Wideband continuously tunable integrated delay line based on cascaded Mach–Zehnder. In: *2018 photonics in switching and computing (PSC)* (pp. 1–3). IEEE, Limassol, Cyprus.
6. Pozar, D. M. (2005). *Microwave engineering* (3rd ed.). New York: Wiley.
7. Hosseini, F., Khalaj-Amir Hosseini, M., & Yazdani, M. (2009). A miniaturized Wilkinson power divider using non uniform transmission line. *Journal of Electromagnetic Waves and Applications, 23*(7), 917–924.
8. Wang, X., Ma, Z., Sakagami, I., Mase, A., & Yoshikawa, M. (2015). Miniaturized Wilkinson power divider with extra coupled line section for compensation. *Microwave and Optical Technology Letters, 57*(8), 1869–1873.
9. Lin, C. M., Su, H. H., Chiu, J. C., & Wang, Y. H. (2007). Wilkinson power divider using microstrip EBG cells for the suppression of harmonics. *IEEE Microwave and Wireless Components Letters, 17*(10), 700–702.
10. Woo, D. J., & Lee, T. K. (2005). Suppression of harmonics in Wilkinson power divider using dual-band rejection by asymmetric DGS. *IEEE Transactions on Microwave Theory and Techniques, 53*(6), 2139–2144.
11. Roshani, S. (2017a). A compact microstrip low-pass filter with ultra wide stopband using compact microstrip resonant cells. *International Journal of Microwave and Wireless Technologies, 9*(5), 1023–1027.
12. Hayati, M., Roshani, S., & Roshani, S. (2013). Miniaturized Wilkinson power divider with nth harmonic suppression using front coupled tapered CMRC. In: *ACES* (Vol. 28, No. 3, pp. 221–227).
13. Roshani, S., Siahkamari, P., & Siahkamari, H. (2017). Compact, harmonic suppressed Gysel power divider with plain structure. *Frequenz, 71*(5–6), 221–226.

14. Roshani, S. (2017b). A Wilkinson power divider with harmonics suppression and size reduction using meandered compact microstrip resonating cells. *Frequenz, 71*(11–12), 517–522.
15. Veysi, M., Ahmadi, A., Karimi, G., & Lalbakhsh, A. (2017). RFID tag design using spiral resonators and defected ground structure. *Radioengineering, 26*(4), 1019–1024.
16. Karimi, G., Lalbakhsh, A., Dehghani, K., & Siahkamari, H. (2015). Analysis of novel approach to design of ultra-wide stopband microstrip low-pass filter using modified u-shaped resonator. *ETRI Journal., 37*(5), 945–950.
17. Karimi, G., Siahkamari, H., Hamedani, F. K., & Lalbakhsh, A. (2015). Design of modified Z-shaped and T-shaped microstrip filter based on transfer function analysis. *Wireless Personal Communications, 82*(4), 2005–2016.
18. Lotfi, S., Roshani, S., Roshani, S., & Gilan, M. S. (2020). Wilkinson power divider with band-pass filtering response and harmonics suppression using open and short stubs. *Frequenz, 74*(5–6), 169–176.
19. Hookari, M., Roshani, S., & Roshani, S. (2020). Design of a low pass filter using rhombus-shaped resonators with an analytical LC equivalent circuit. *Turkish Journal of Electrical Engineering & Computer Sciences., 28*(2), 865–874.
20. Roshani, S., & Roshani, S. (2020). Design of a compact LPF and a miniaturized Wilkinson power divider using aperiodic stubs with harmonic suppression for wireless applications. *Wireless Networks., 26*(2), 1493–1501.
21. Heydari, M., Rostami, P., & Roshani, S. (2019). Design of a modified Wilkinson power divider with size reduction and harmonics suppression using triangle-shaped resonators. *Wireless Personal Communications, 109*(3), 1571–1579.
22. Golestanifar, A., & Roshani, S. (2019). Design of an ultra-sharp composite low-pass filter using analytical method. *Analog Integrated Circuits and Signal Processing., 100*(2), 249–255.
23. Lalbakhsh, A., Ghaderi, A., Mohyuddin, W., Simorangkir, R. B., Bayat-Makou, N., Ahmad, M. S., et al. (2020). A compact C-B and bandpass filter with an adjustable dual-band suitable for satellite communication systems. *Electronics, 9*(7), 1088.
24. Karimi, G., Amirian, M., Lalbakhsh, A., & Ranjbar, M. (2019). A new microstrip coupling system for realization of a differential dual-band bandpass filter. *AEU-International Journal of Electronics and Communications, 99,* 186–192.
25. Amirian, M., Karimi, G., Lalbakhsh, A., & Bayati, M. S. (2015). Compact differential bandpass filter with a narrow notched band using APCL structure suitable for UWB application. *Microelectronics Journal, 46*(9), 869–874.
26. Zhan, W. L., & Zhao, X. L. (2017). Compact filtering power divider with harmonic suppression. *Journal of Electromagnetic Waves and Applications, 31*(3), 243–249.
27. Wang, Y., Zhang, X. Y., Liu, F. X., & Lee, J. C. (2017). A compact bandpass Wilkinson power divider with ultra-wide band harmonic suppression. *IEEE Microwave and Wireless Components Letters, 27*(10), 888–890.
28. Jamshidi, M., Lalbakhsh, A., Lotfi, S., Siahkamari, H., Mohamadzade, B., & Jalilian, J. (2020). A neuro-based approach to designing a Wilkinson power divider. *International Journal of RF and Microwave Computer-Aided Engineering, 30*(3), e22091.
29. Jamshidi, M., Lalbakhsh, A., Talla, J., Peroutka, Z., Hadjilooei, F., Lalbakhsh, P., et al. (2020). Artificial intelligence and COVID-19: Deep learning approaches for diagnosis and treatment. *IEEE Access, 8,* 109581–109585.
30. Zirak, A. R., & Roshani, S. (2016). Design and modeling of RF power amplifiers with radial basis function artificial neural networks. *International Journal of Advanced Computer Science and Applications, 7*(6), 227–231.
31. Du, Z. X., Zhang, X. Y., Wang, K. X., Kao, H. L., Zhao, X. L., & Li, X. H. (2016). Unequal Wilkinson power divider with reduced arm length for size miniaturization. *IEEE Transactions on Components, Packaging and Manufacturing Technology, 6*(2), 282–289.
32. Li, J. L., Wang, H. Z., Wang, J. P., Gao, S. S., Yang, X. S., & Shao, W. (2016). Miniaturized Wilkinson power dividers with harmonic suppressions. *Electromagnetics, 36*(3), 157–166.
33. Mirzavand, R., Honari, M. M., Abdipour, A., & Moradi, G. (2013). Compact microstrip Wilkinson power dividers with harmonic suppression and arbitrary power division ratios. *IEEE Transactions on Microwave Theory and Techniques, 61*(13), 61–68.
34. Hayati, M., & Roshani, S. (2013) A novel Wilkinson power divider using open stubs for the suppression of harmonics. In: *ACES* (Vol. 28, No. 6).

Masoud Heydari was born in Kermanshah, Iran in 1992. He received his B.Sc. and M.Sc. degrees in Electronics Engineering from Islamic Azad University, Kermanshah, Iran in 2015 and 2017, respectively. He joined Young Researchers and Elite Club in 2017. His current research includes microwave passive circuits and RF integrated circuit design.

Saeed Roshani received the B.Sc. degree in Electrical Engineering from Razi University, Kermanshah, Iran in 2008; M.Sc. degree in Electrical Engineering from Shahed University, Tehran, Iran in 2011; and Ph.D. in Electrical Engineering from Razi University in 2015. He performed opportunity research program in Amirkabir University of Technology (Tehran Polytechnics) Iran, in 2014–2015. He graduated as the best student of his country among all students of Iran on 2015 and Awarded by the First Vice President and Science, Research & Technology Minister. He is currently an Assistant Professor in the Department of Electrical Engineering at Islamic Azad University, Kermanshah, Iran. He has published more than 70 papers in ISI Journals and Conferences. His research interest includes the microwave and millimeter wave devices and circuits, low-power and low-size integrated circuit design.